



Preliminary Investigation of Surface Treatments to Enhance the Wear Resistance of 60-Nitinol

Malcolm K. Stanford
Glenn Research Center, Cleveland, Ohio

NASA STI Program . . . in Profile

Since its founding, NASA has been dedicated to the advancement of aeronautics and space science. The NASA Scientific and Technical Information (STI) Program plays a key part in helping NASA maintain this important role.

The NASA STI Program operates under the auspices of the Agency Chief Information Officer. It collects, organizes, provides for archiving, and disseminates NASA's STI. The NASA STI Program provides access to the NASA Technical Report Server—Registered (NTRS Reg) and NASA Technical Report Server—Public (NTRS) thus providing one of the largest collections of aeronautical and space science STI in the world. Results are published in both non-NASA channels and by NASA in the NASA STI Report Series, which includes the following report types:

- **TECHNICAL PUBLICATION.** Reports of completed research or a major significant phase of research that present the results of NASA programs and include extensive data or theoretical analysis. Includes compilations of significant scientific and technical data and information deemed to be of continuing reference value. NASA counter-part of peer-reviewed formal professional papers, but has less stringent limitations on manuscript length and extent of graphic presentations.
- **TECHNICAL MEMORANDUM.** Scientific and technical findings that are preliminary or of specialized interest, e.g., “quick-release” reports, working papers, and bibliographies that contain minimal annotation. Does not contain extensive analysis.
- **CONTRACTOR REPORT.** Scientific and technical findings by NASA-sponsored contractors and grantees.
- **CONFERENCE PUBLICATION.** Collected papers from scientific and technical conferences, symposia, seminars, or other meetings sponsored or co-sponsored by NASA.
- **SPECIAL PUBLICATION.** Scientific, technical, or historical information from NASA programs, projects, and missions, often concerned with subjects having substantial public interest.
- **TECHNICAL TRANSLATION.** English-language translations of foreign scientific and technical material pertinent to NASA's mission.

For more information about the NASA STI program, see the following:

- Access the NASA STI program home page at <http://www.sti.nasa.gov>
- E-mail your question to help@sti.nasa.gov
- Fax your question to the NASA STI Information Desk at 757-864-6500
- Telephone the NASA STI Information Desk at 757-864-9658
- Write to:
NASA STI Program
Mail Stop 148
NASA Langley Research Center
Hampton, VA 23681-2199

NASA/TM—2016-219121



Preliminary Investigation of Surface Treatments to Enhance the Wear Resistance of 60-Nitinol

Malcolm K. Stanford
Glenn Research Center, Cleveland, Ohio

National Aeronautics and
Space Administration

Glenn Research Center
Cleveland, Ohio 44135

July 2016

Trade names and trademarks are used in this report for identification only. Their usage does not constitute an official endorsement, either expressed or implied, by the National Aeronautics and Space Administration.

This work was sponsored by the Fundamental Aeronautics Program at the NASA Glenn Research Center.

Level of Review: This material has been technically reviewed by technical management.

Available from

NASA STI Program
Mail Stop 148
NASA Langley Research Center
Hampton, VA 23681-2199

National Technical Information Service
5285 Port Royal Road
Springfield, VA 22161
703-605-6000

This report is available in electronic form at <http://www.sti.nasa.gov/> and <http://ntrs.nasa.gov/>

Preliminary Investigation of Surface Treatments to Enhance the Wear Resistance of 60-Nitinol

Malcolm K. Stanford
National Aeronautics and Space Administration
Glenn Research Center
Cleveland, Ohio 44135

Abstract

The use of protective surface treatments on 60-Nitinol (60wt%Ni-40wt%Ti) was studied. Various nitriding techniques as well as a (Ti,Al)N coating were evaluated visually, microscopically, and by hardness and scratch testing. The chemical composition of the surface treatments was investigated by x-ray techniques. The results indicate that very hard (greater than 1,000 HK) and adherent surface layers can be produced on 60-Nitinol. Further work is needed to determine the tribological properties of these surface treatments in relevant operating environments.

Background

60-Nitinol (60wt%Ni-40wt%Ti) is an intermetallic material with a unique combination of properties. This material is immune to aqueous corrosion and is compatible with conventional oil-based lubricants (Refs. 1 to 3). It has a low apparent elastic modulus, high elastic limit and is hardenable through a relatively simple heat treatment to a hardness value equivalent to that of bearing steels (Refs. 2 to 5). This blend of physical properties makes 60-Nitinol a candidate for a number of aerospace applications including gears, bearings and other implements (Refs. 3 to 5).

Although 60-Nitinol performs well in lightly-loaded lubricated apparatuses, the wear behavior of this material in non-lubricated systems has been essentially unexplored. The ability to apply a surface treatment to increase the surface hardness and concomitant wear resistance of 60-Nitinol would enable the use of this material in lightly-lubricated or dry-running tribological systems like those found in tooling, seals, food processing equipment, cutlery and personal appliances even including jewelry. The purpose of this study was to evaluate the physical characteristics of 60-Nitinol after application of several surface treatments. These results will provide an indication of the feasibility of the use of 60-Nitinol in lightly-lubricated and dry-running tribological systems.

Experimental Procedures

Induction skull melted 60-Nitinol was procured from Flowserve Corporation (Dayton, Ohio). The nominal composition of the material was 60wt%Ni-40wt%Ti with the following impurities (in parts per million): O (680), Fe (130), Al (200), N (40), Co (30), Cr (20). Disk-shaped coupons (approximately 25 mm in diameter by 6 mm thick) were machined from the material by wire electrical discharge machining. The coupons were hardened by heat treating in air for 2 h at 1050 °C followed by water quenching. This heat treatment is designed to harden the material to at least approximately 500 HV (~50 Rockwell C) for increased wear resistance. Previous studies have shown that subsequent heating at approximately 400 °C for 30 to 60 min can further increase hardness but prolonged exposure to elevated temperatures results in over-aging and softening of the material (Ref. 6). Moreover, heating the material at 1050 °C and allowing it to furnace cool results in annealed material that has hardness of approximately 350 HV (~35 Rockwell C). Therefore, the effects of substrate heating during surface treatment on hardness should be considered.

The coupons were ground and polished on one side to a mirror finish ($R_a < 0.2 \mu\text{m}$), as shown in Figure 1, prior to shipment to commercial vendors for surface treatment. The surface treatments used in this study are listed in Table 1. Treatment A was a (Ti,Al)N coating applied by physical vapor deposition (PVD) (Refs. 7 and 8). This surface treatment was applied by Hohman Plating & Manufacturing (Dayton, Ohio). During the deposition process, the substrate temperature rises to approximately 500 °C for 3 h. Treatment B was a gas nitriding surface treatment (Ref. 9). During this process, the substrate was held at 380 °C for 30 min in a nitrogenous atmosphere to promote the growth of a nitride-rich surface layer. Treatment C was an activated gas nitriding treatment where the substrate was heated to 570 °C for approximately 30 min in a nitrogenous atmosphere (Refs. 10 and 11). The nitriding activation potential, K_n , is defined as

$$K_n = \frac{p_{NH_3}}{p_{H_2}^{3/2}}$$

where p_{NH_3} is the partial pressure of ammonia and $p_{H_2}^{3/2}$ is the partial pressure of hydrogen, was $2.5 \text{ atm}^{-1/2}$ (Refs. 12 and 13). Treatments D and E are nitrided by plasma discharge processes (Refs. 9 and 14). These processes modify the conventional gas nitriding process by generating nitrogen ions in a plasma and then accelerating them into the substrate to create nitrides near the surface. Since the acceleration of ions is unidirectional, the resulting treatment is essentially line-of-sight. Treatment D is a *direct plasma nitriding* treatment. In this process, the substrate was heated to 540 °C in a partial pressure mixture of nitrogen, hydrogen and argon at a base pressure of 2.45 mbar. A plasma is formed with a voltage potential of 550 V pulsed for 40 μsec . Treatment E used an *indirect plasma nitriding* treatment where the substrate was heated to 730 °C in an atmosphere with a partial pressure of nitrogen at a base pressure of 2.6 mbar. Surface treatments B to E were applied by Advanced Heat Treat Corporation (Monroe, Michigan).

The treated surfaces were polished starting with a 0.5 μm diamond suspension on a vibratory polisher followed by 0.05 μm colloidal silica suspension. Cross sections of the surface treatments and bulk material (perpendicular to the treated surfaces) were prepared for microscopy and testing using standard metallographic techniques (Ref. 15). This procedure began with plane grinding with a coarse SiC abrasive disk and ended with vibratory polishing on 0.05 μm colloidal silica. The thickness of each surface treatment was measured using calibrated image analysis software. Each captured image pixel corresponded to approximately 0.5 μm vertically and horizontally. The average and standard deviation of twenty thickness measurements per treated specimen was reported.

Hardness testing and scratch testing were used to evaluate the surface treatments in this study. Hardness is the resistance of a material to penetration by an indenter. In this study, this property will also be used as a preliminary indicator of its wear resistance. Microindentation hardness was measured for the bulk substrate material with a Vickers indenter using a 200 gf load, based on a standard test specification (Ref. 16). The average hardness measured at five locations was reported. Due to the thinness of the layers, the hardness of surface treatments A, B, and C were measured using a Knoop indenter using a 50 gf load. Compared to the regular pyramidal shape of the Vickers indenter, the Knoop indenter has an elongated pyramidal shape that was developed for testing thin layers (Refs. 16 and 17). The case layers created by surface treatments D and E, however, were too thin for reliable microindentation hardness testing.

Scratch testing, where a load is applied to a stylus as it is dragged across a surface, is also a commonly used evaluation for coatings and surface treatments (Ref. 18). This test can be used as an indication of the adhesion of a surface layer to a substrate, since a brittle or non-adherent surface treatment will crack and expose the substrate. A CSEM Automatic Scratch-Tester with a Revetest apparatus was used to perform single-pass scratch testing on the treated surfaces. The instrument used a stylus with a conically-tipped scratching element. The normal force on the stylus increased from 10 to 80 N over the length of the scratch channel. The path traversed by the stylus was approximately 3.3 mm.

The microstructures of the specimens, perpendicular to the treated surface, were observed using optical or scanning electron microscopy. Scanning electron microscopy (SEM) was used to observe the scratch scar on each specimen and the integrity of the surface treatment was determined by visual observation. Energy dispersive x-ray spectroscopy (EDS) was used to examine the chemical composition of selected specimen surfaces. The crystalline phases present at and near the surface of each treated specimen were identified by x-ray diffraction (XRD) using Cu K α radiation.

Results and Discussion

Visual Observations

Images of specimens after each surface treatment are shown in Figure 2. Surface treatment A appears smooth (following the surface finish of the substrate) though slightly dull and dark grey. Treatments B and C had matte light grey and medium grey appearances, respectively. Treatment D had a reddish-gold color with a somewhat mottled surface finish. Treatment E left a yellow-gold, diffuse surface finish. After fine polishing, the surface roughness of each surface treatment was noticeably lower, resulting in higher reflectivity. Images of each surface treatment after polishing are shown in Figure 3. Treatment A had a smooth and reflective medium grey surface. Treatments B and C had a somewhat reflective surface with a faintly golden hue. Treatments D and E had deeply lustrous finishes with yellowish-golden hues. Previous studies have demonstrated that surface treatments that produce TiN can vary in color from grey to gold to brownish red depending on the amount of nitrogen available to the substrate during the surface treatment (Refs. 19 and 20). These considerations would be most relevant if these treatments were used for aesthetic purposes.

Microstructure and Composition

Photomicrographs of cross sections of each specimen are shown in Figure 4. The surface treatment is positioned near the top of each image with the substrate beneath. In the case of the (Ti,Al)N coated and the plasma nitrided specimens, the treated surfaces had to be nickel plated prior to mounting and polishing for adequate edge-retention. The approximate thickness of each surface treatment is listed in Table 1. The layers deposited plasma nitriding methods (treatments D and E) had less uniform thickness, resulting in relatively large statistical variation compared to the average thickness values. This is especially true for surface treatment D, which is possibly the reason this surface treatment had the mottled as-deposited appearance noted previously.

An image of the (Ti,Al)N coating, visualized approximately 45° from normal to the coating is shown in Figure 5. In the image, the coating resembles a peninsular land mass with white mounds and similarly-sized depressions. The substrate can be seen beneath the coating. Analysis of the coating confirmed that it was composed of N, Ti, and Al. X-ray diffraction identified the crystalline phase of the coating as Ti-Al_{2.76}-Ni_{0.24} (at.%). A cross section of the coating is shown in Figure 6. EDS analysis of the cross section indicates that the composition of the coating varies in the concentrations of Ni, Al and N within the coating. There is a nitrogen-rich layer just above the Ni-Ti substrate but further work would be necessary to determine its stoichiometry due to the interference between N and Ti x-ray peaks.

An SEM image of a specimen with gas nitrided surface treatment B is shown in Figure 7. XRD detected the presence of cubic TiN that was formed on the surface of this specimen during the surface treatment (see Table 1). Further work would be needed to characterize the apparent voids within the case layer, ostensibly formed during the nitriding process. XRD detected the presence of TiN as well as cubic Ni, which may indicate a depletion of the Ti from the Ni-Ti matrix, resulting in monolithic Ni.

Figure 8 is an SEM image of a cross-section of a specimen after treatment C. Based on the EDS analyses, the darker regions are titanium-rich, while the lighter regions are nickel-rich. As with treatment B, XRD detected TiN and cubic Ni. Also similar to treatment B, voids can be seen within the case layer and further work would be needed to determine what affect, if any, they have on the performance of the surface treatment.

EDS analysis of surface treatment D (direct plasma nitriding) is shown in Figure 9. As mentioned previously, the treatment layer varies in thickness. Based on the EDS spectra (Figs. 9(b) and (c)), it is rich in nitrogen, nickel and titanium, which, according to x-ray diffraction (see Table 1), is present mainly in the form of TiN and Ni₃Ti, a precipitate phase in Ni-rich Ni-Ti compounds. The carbon detected by EDS is from the metallographic mounting media and not present in the specimen. The surface treatment is thin enough that the x-rays from the diffractometer pass through to the substrate.

A cross section of a specimen given surface treatment E (indirect plasma nitriding) was analyzed by EDS, as shown in Figure 10. The treated area is rich in nickel and titanium, as would be expected, but this area has a slightly higher titanium concentration than the substrate. X-ray diffraction detected TiN, as well as the expected crystalline phases present in the substrate (NiTi, Ni₃Ti, and NiTi₂).

Hardness

Hardness values of control specimens after the hardening heat treatment (673 HV \approx 59 Rockwell C) and after annealing (366 HV \approx 37 Rockwell C) are compared to those of the cross-sectioned substrates after each of the studied surface treatments in Figure 11. Treatments A and E reduced the hardness of the substrate noticeably, suggesting partial annealing of the substrate during the surface treatment process. Reduction of the substrate hardness would not render a surface treatment ineffective, however, if some other benefit (such as increased surface hardness) were obtained. It is also possible that the surface treatments considered in this study could be optimized for 60-Nitinol to prevent annealing, though that is beyond the scope of the present work. In any case, treatments B, C and D resulted in little appreciable softening of the substrate.

The hardness of surface treatment A, measured on the cross-sectioned surface treatment, was approximately 374 HK. The gas nitriding treatments (surface treatments B and C) generated markedly higher hardness values (1,018 and 1,094 HK, respectively). As mentioned previously, since the plasma nitrided surface treatments (treatments D and E) were too thin for hardness testing of the cross section, hardness of these treatments was measured on the polished, treated surface (perpendicular to the surface). Surface treatment D had a hardness of 574 HV, while surface treatment E had a hardness of 365 HV. These values are not comparable to the hardness measurements that were made parallel to the surface because the compliance of the substrate has a great influence on the measurement but they are reported as mere indicators of the integrity of the surface layer.

Scratch Testing

SEM photomicrographs of the scratch channel profiles from surface treatments A to E are shown in Figures 12 to 17. The scratch channel for the (Ti,Al)N coating, shown in Figure 12, showed signs of separation and delamination after the stylus had traversed approximately 3,178 μ m, corresponding to a load of approximately 78 N, calculated with a linear correlation. EDS analysis of regions near the end of the scratch (see Figs. 12(b) to (e)) confirmed coating spallation where high concentrations of Ni were detected at cracks in the surface layer.

The scratch channel for surface treatment B, shown in Figure 13, begins to show cracking approximately 1,099 μ m from the start of the channel, corresponding to a load of approximately 33 N. The scratch channel for surface treatment C was examined by SEM, as shown in Figure 14. The surface treatment showed cracking approximately 120 μ m from the start of the channel, corresponding to a load of approximately 23 N. Cracking is an indication of the brittleness of the surface layer. There was no decohesion from the base material, nevertheless, which indicates that the surface layer is fairly tenacious.

The scratch channel on surface treatment D, shown in Figure 15, remains adherent to the substrate and shows indications of plastic deformation at the end of the scratch channel (note the ridge of displaced material). As shown in Figure 16, the EDS dot mapping at the end of the wear channel indicate that the disturbed material is composed of evenly distributed Ni, Ti, and N with no indications of cracking. Similarly, surface treatment E appears to remain adherent to the substrate until the end of the scratch channel where there is some separation along the edge of the channel, which can be seen in Figure 17. For comparison, a baseline scratch channel profile on a hardened (673 HV), polished, and untreated 60-NiTi surface is shown in Figure 18. This scratch channel shows scoring that runs parallel to the direction of the scratch. There is a mass of displaced material at the end of the scratch channel, which indicates abrasive wear of 60-Nitinol.

It should be noted that, since the surface roughness of the treated specimens was not controlled and the coefficient of friction between the scratching element and the treated specimen was not measured, these results only represent an initial screening of the integrity of these surface treatments. Further work is needed to determine their tribological properties in relevant operating environments.

Summary

The purpose of this study was to perform a preliminary investigation of surface treatments for 60-Nitinol to assess the feasibility of further developmental work. The major findings from this study are summarized below.

Surface treatment A (the Ti-Al-N coating) had a grey appearance and was primarily composed of Ti-Al_{2.76}-Ni_{0.24} (at. %). This coating had relatively low hardness (374 HK_{0.05}) but adhered to the substrate at up to a scratch test load of 50N. The coating process partially annealed the substrate, reducing its hardness to 460 HV_{0.2}. The nitriding techniques produced surface layers of various golden hues due to the formation of TiN. Gas nitriding generated case layers that were hard (1,018 to 1,094 HK_{0.05} for surface treatments C and B, respectively) without appreciable softening of the substrate. However, due to their brittleness, the cases cracked at moderate loads (23 to 33 N). Plasma nitriding produced ductile surfaces that adhered to the substrate up to approximately 80 N. Direct plasma nitriding did not soften the substrate substantially but indirect plasma nitriding softened the substrate to approximately 348 HV. Further work is needed to measure the hardness of the plasma nitrided surfaces, which were too thin for microindentation hardness testing of their cross sections.

These results are encouraging and, based on this study, further development of surface treatments for 60-Nitinol is warranted. Based on the results of this study, it would be useful to investigate the friction and wear behavior of the gas nitrided coatings at low loads and the direct plasma nitrided coating at both low and moderate loads. The tribological behavior of these treatments should be studied under both lubricated and unlubricated conditions. The availability of this technology would enable development of instruments such as cutting tools and other wear-resistant apparatuses that also employ the beneficial properties of 60-Nitinol.

References

1. S.V. Pepper, C. DellaCorte, R. Noebe, D.R. Hull and G. Glennon, "NITINOL 60 as a Material for Spacecraft Triboelements," presented at the ESMATS 13 Conference, Vienna, Austria, September 2009.
2. C. DellaCorte, S.V. Pepper, R. Noebe, D.R. Hull, G. Glennon, "Intermetallic Nickel-Titanium Alloys for Oil-Lubricated Bearing Applications," NASA/TM—2009-215646, March 2009, National Technical Information Service, Springfield, VA.
3. W.J. Buehler and F.E. Wang, "A Summary of Recent Research on the Nitinol Alloys and their Potential Application in Ocean Engineering," *Ocean Engineering*, Vol. 1, pp. 105–120, 1968.

4. W.J. Buehler, "Intermetallic Compound Based Materials for Structural Applications," in The Seventh Navy Science Symposium: Solution to Navy Problems through Advanced Technology, May 14, 15, 16, 1963, U.S. Naval Aviation Medical Center, Pensacola, Florida. Vol. 1, Office of Naval Research, Arlington, VA, 16 May 1963.
5. C. DellaCorte, R. Noebe, M.K. Stanford and S.A. Padula, "Resilient and Corrosion-Proof Rolling Element Bearings Made From Superelastic Ni-Ti Alloys for Aerospace Mechanism Applications," NASA/TM—2011-217105, National Technical Information Service, Springfield, VA.
6. B.C. Hornbuckle, R.D. Noebe, and G.B. Thompson, Influence of Hf Solute Additions on the Precipitation and Hardenability in Ni-rich NiTi Alloys, *Journal of Alloys and Compounds*, Vol. 640, pp. 449–54, 2015.
7. D.M. Mattox, "Growth and Growth-Related Properties of Films Formed by Physical Vapor Deposition," in *ASM Handbook*, Vol. 5: Surface Engineering, 1994, pp. 538–55.
8. T. Leyendecker, O. Lemmer, S. Esser, and J. Ebberink, "The development of the PVD coating TiAlN as a commercial coating for cutting tools," *Surface and Coatings Technology*, 48 (1991) 175–78.
9. G. Krauss, "Physical Metallurgy and the Heat Treatment of Steel," in *Metals Handbook Desk Edition*, Chapter 28: Heat Treating, American Society for Metals, Metals Park, OH, 1985.
10. E.J. Mittemeijer, "Fundamentals of Nitriding and Nitrocarburizing," in *ASM Handbook*, Volume 4A, Steel Heat Treating Fundamentals and Processes, J. Dossett and G.E. Totten, editors, 2013.
11. L. Liu, F. Ernst, G.M. Michal, and A.H. Heuer, "Surface Hardening of Ti Alloys by Gas-Phase Nitridation: Kinetic Control of the Nitrogen Surface Activity," *Metallurgical and Materials Transactions A*, 36A, September 2005, pp. 2429–2434.
12. X. Wang, "Activated Atmosphere Case Hardening of Steels," Ph.D. dissertation, Worcester Polytechnic Institute, 2011.
13. M. Yang, "Nitriding – Fundamentals, Modeling and Process Optimization," Ph.D. dissertation, Worcester Polytechnic Institute, 2012.
14. E. Rolinski, "Mechanism of high-temperature plasma nitriding of titanium," *Materials Science and Engineering*, Vol. 100, pp. 193–99, 1988.
15. ASTM Test Method E 3-11. 2014. Standard Guide for Preparation of Metallographic Specimens. Annual Book of ASTM Standards, Vol. 03.01. West Conshohocken, PA: American Society for the Testing of Metals.
16. ASTM Test Method E 384-11^{e1}. 2011. Standard Test Method for Knoop and Vickers Hardness of Materials. Annual Book of ASTM Standards, Vol. 03.01. West Conshohocken, PA: American Society for the Testing of Metals.
17. F. Knoop, C.G. Peters and W.B. Emerson, "A Sensitive Pyramidal-Diamond Tool for Indentation Measurements," *Journal of Research of the National Bureau of Standards*, Vol. 23, No. 1, 1939, pp. 39–61.
18. S. Jacobsson, M. Olsson, P. Hedenqvist and O. Vingsbo, "Scratch Testing," in *ASM Handbook*, Vol. 18: Friction, Lubrication, and Wear Technology, Scott D. Henry, ed., 1992, pp. 430–437.
19. P. Roquiny, F. Bodart and G. Terwagne, "Colour control of titanium nitride coatings produced by reactive magnetron sputtering at temperatures less than 100 °C," *Surface and Coatings Technology*, Vol. 116–119, 1999, pp. 278–283.
20. G. Reiners, H. Hantsche, H.A. Jehn, U. Kopacz, and A. Rack, "Decorative properties and chemical composition of hard coatings," *Surface and Coatings Technology*, Vol. 54/55, 1992, pp. 273–278.

TABLE 1.—SURFACE TREATMENT DATA

Designation	Surface treatment	Thickness, μm	Crystalline phases present	Hardness	Damage load
A	(Ti,Al)N PVD coating	12.2 \pm 2.0	Ti-Al _{2.76} -Ni _{0.24} , monoclinic and cubic NiTi, rhombohedral Ni ₄ Ti ₃ , hexagonal Ni ₃ Ti	373.6 \pm 18.9 HK _{0.05}	78 N
B	Gas nitriding ²	58.7 \pm 1.8	Cubic TiN, cubic Ni	1,018 \pm 315 HK _{0.05}	29 N
C	Activated gas nitriding	67.0 \pm 4.1	Cubic TiN, cubic Ni	1,094 \pm 397 HK _{0.05}	33 N
D	Direct plasma nitriding	6.0 \pm 3.5	hexagonal and cubic TiN, Ni ₃ Ti	573.6 \pm 15.0 HV _{0.2} *	>80 N
E	Indirect plasma nitriding	5.6 \pm 1.2	Cubic TiN, cubic NiTi, hexagonal Ni ₃ Ti, cubic NiTi ₂	316.8 \pm 11.0 HV _{0.2} *	\geq 80 N

*Due to the thinness of the coating, these measurements were made perpendicular to treated surface.

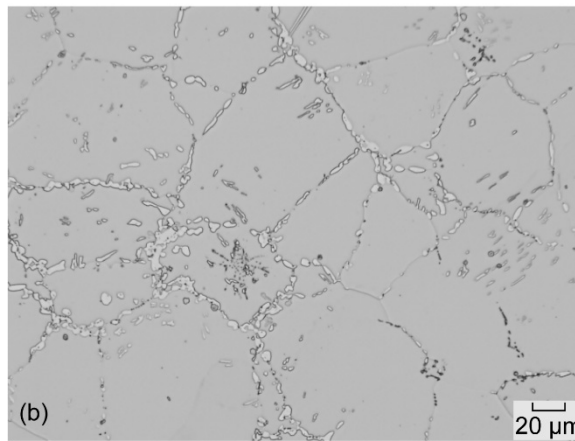
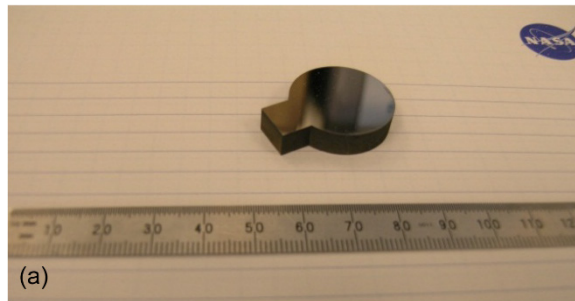


Figure 1.—(a) Photograph of untreated (60-Nitinol substrate) specimen and (b) image of substrate microstructure (swab etched with an aqueous solution of 1 vol% HF and 10 vol% HNO₃).

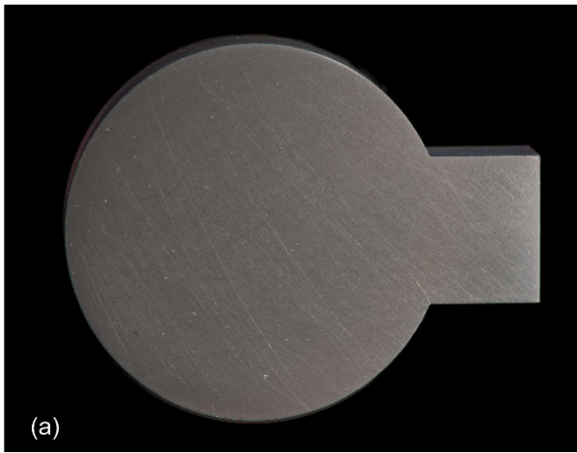


Figure 2.—Photographs of the as-deposited treated surfaces after surface treatments (a) A, (b) B, (c) C, (d) D, and (e) E.

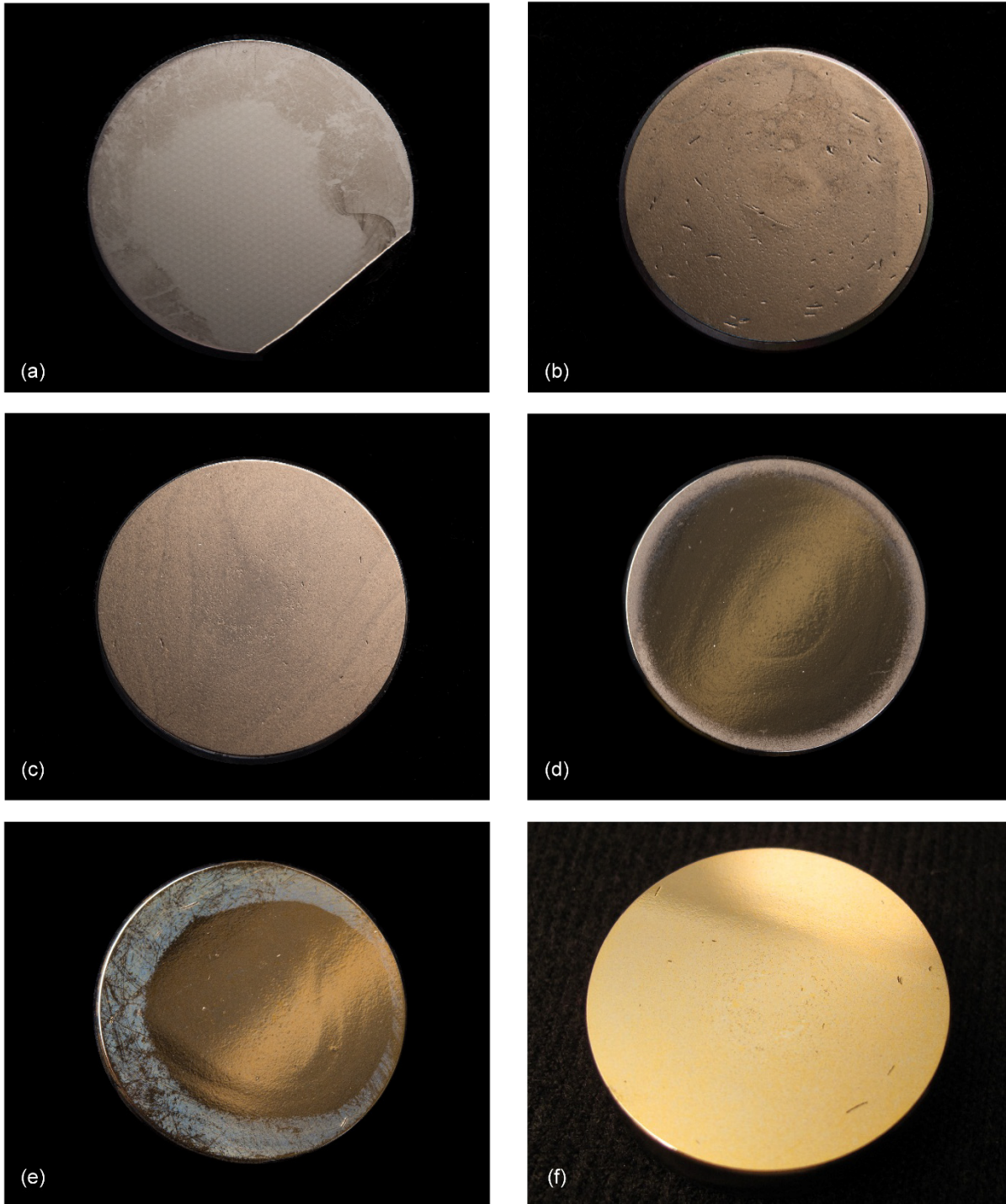


Figure 3.—Photographs of the polished treated surfaces after surface treatments (a) A, (b) B, (c) C, (d) D and (e) to (f) E. The light haze around the edge of the disk in 3(e) is merely residue from the polishing process, which has been removed in 3(f).

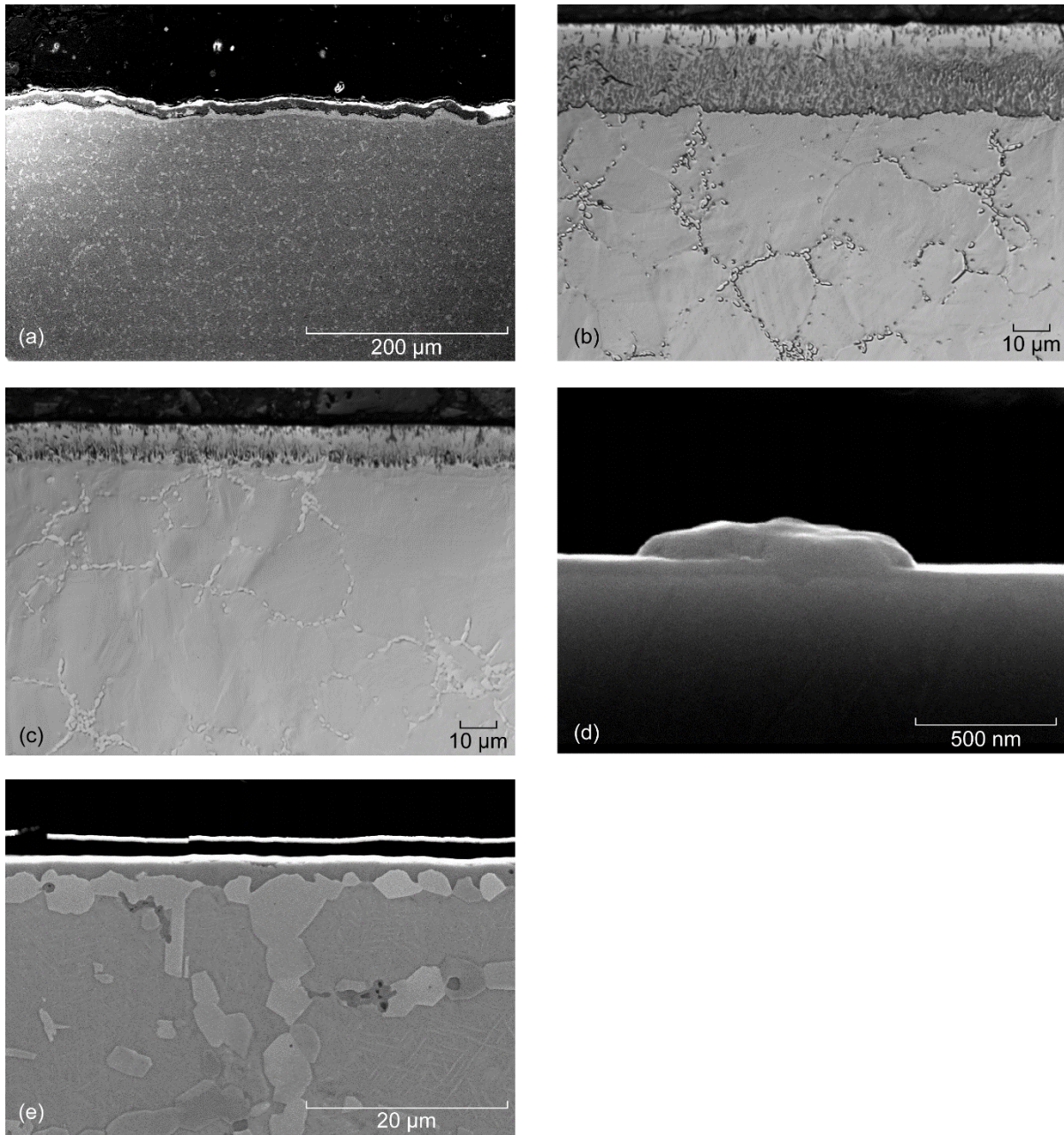


Figure 4.—Cross sectional photomicrographs of each of the studied surface treatments: (a) surface treatment A (Ti-Al-N coating), (b) surface treatment B (gas nitriding), (c) surface treatment C (activated gas nitriding), (d) surface treatment D (direct plasma nitriding) and (e) indirect plasma nitriding.

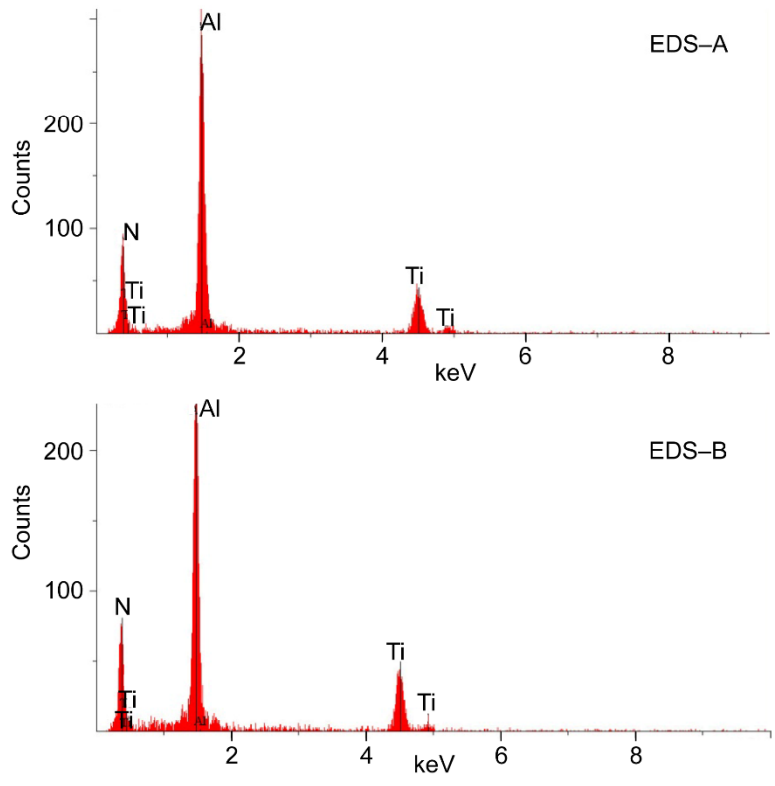
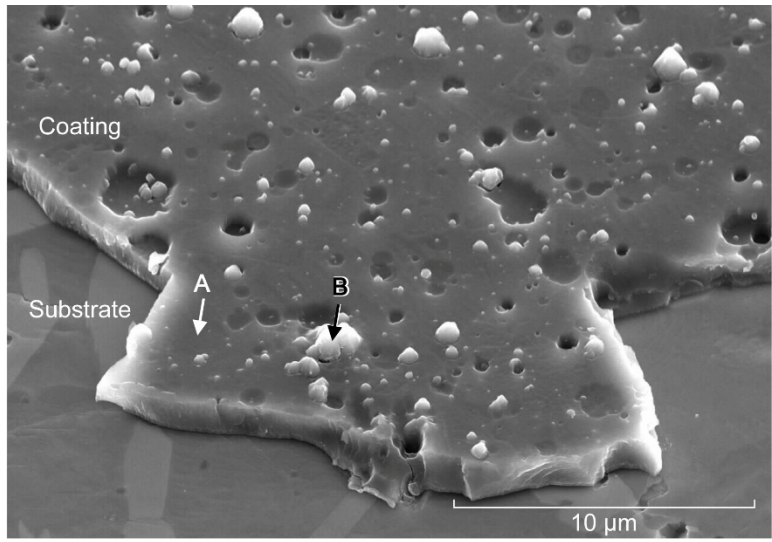


Figure 5.—(Ti,Al)N coating on 60-Nitinol substrate with EDS analysis of composition in locations labeled A and B.

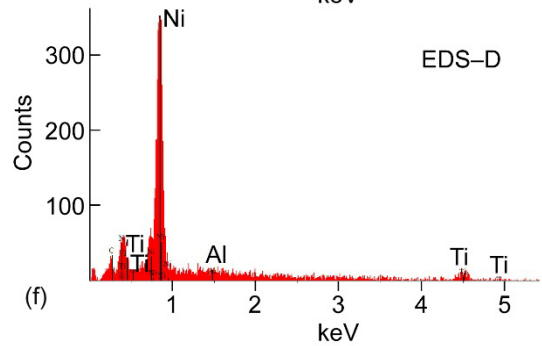
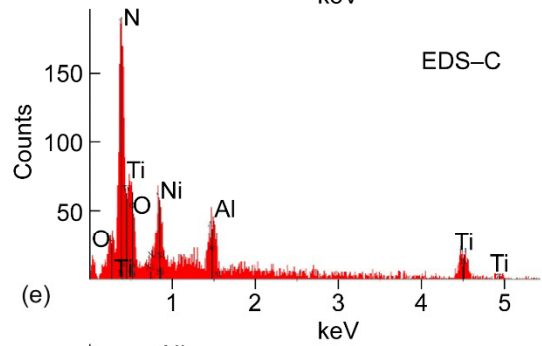
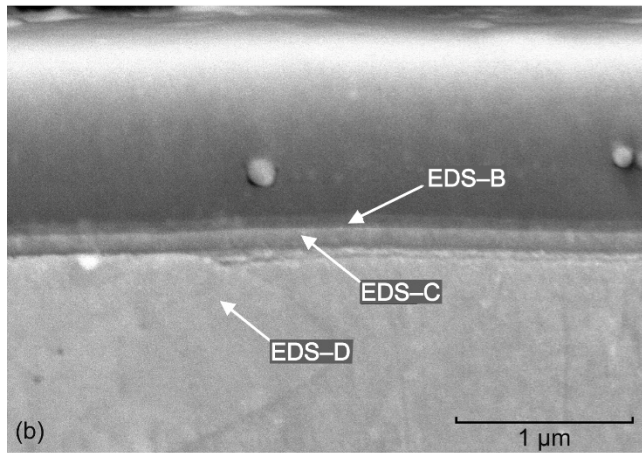
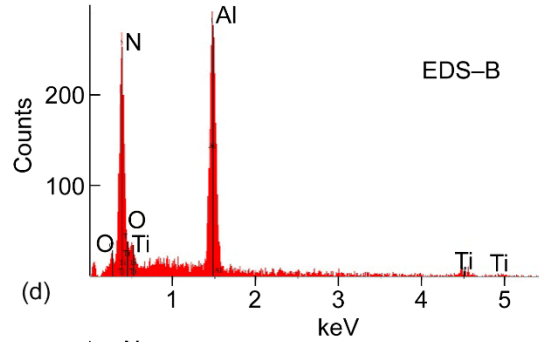
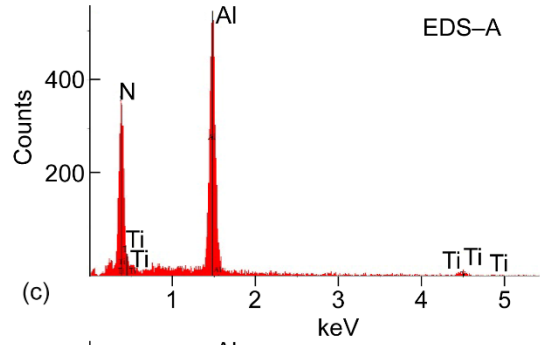
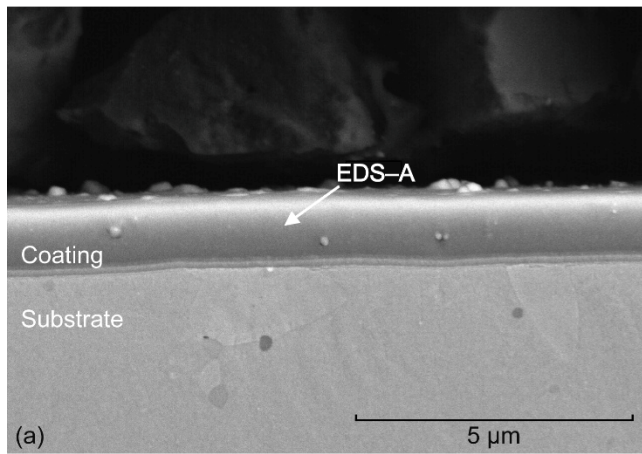


Figure 6.—SEM photomicrographs at (a) lower- and (b) higher-magnification showing the coating-substrate interface resulting from surface treatment A with areas indicating EDS analyses and the resulting EDS spectra (c) to (f).

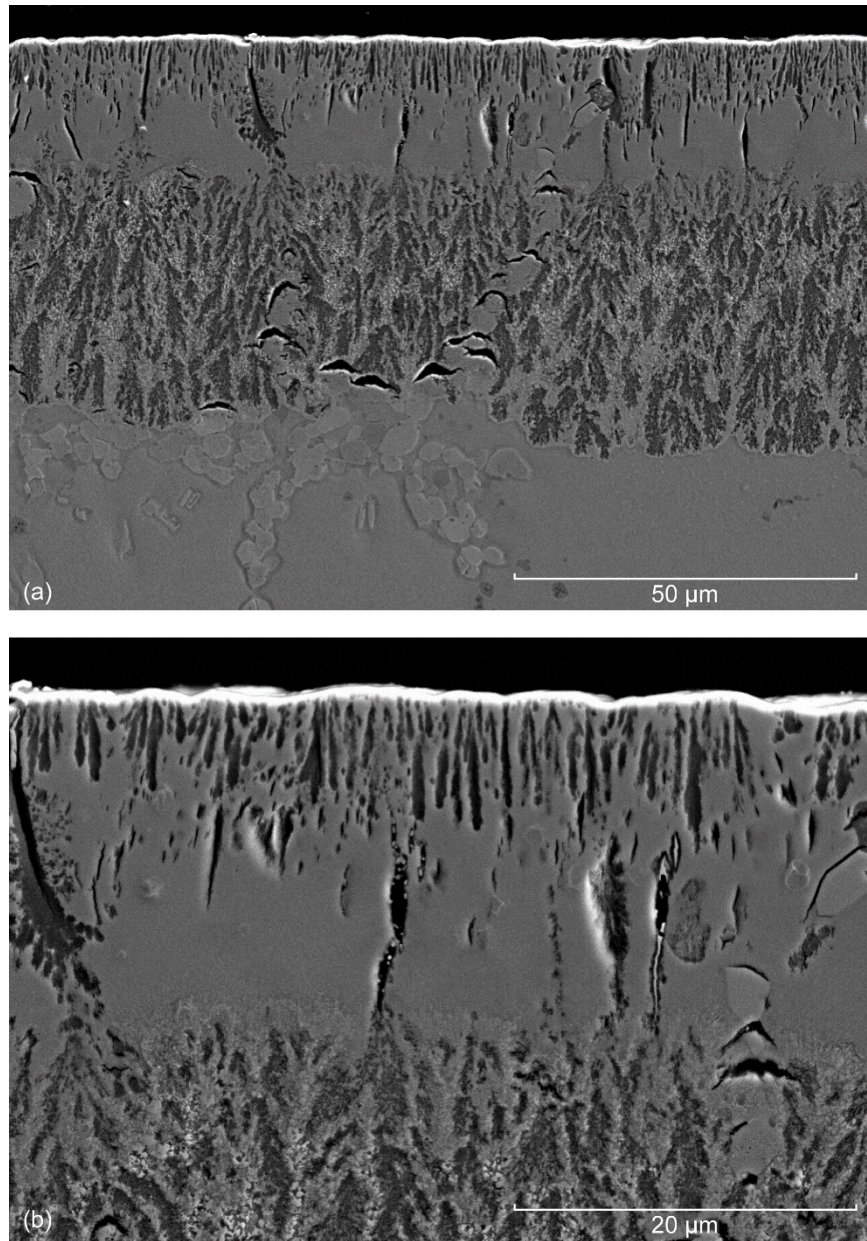


Figure 7.—SEM photomicrographs showing cross section of 60-Nitinol substrate after gas nitriding (surface treatment B) at (a) lower- and (b) higher-magnification.

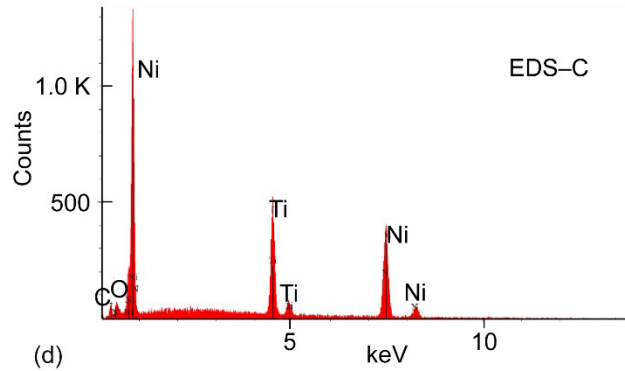
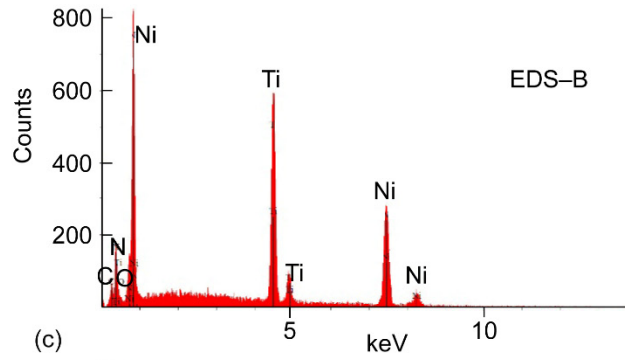
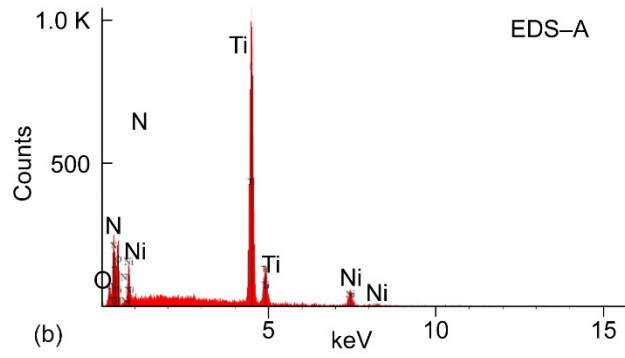
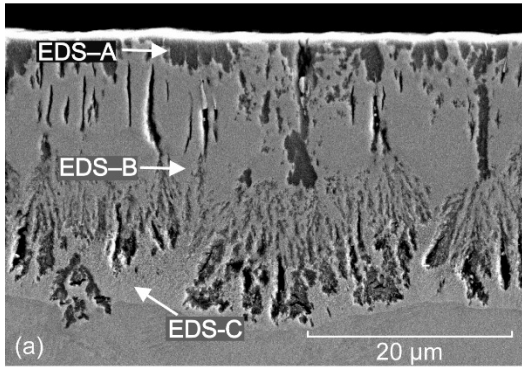


Figure 8.—SEM photomicrograph of cross section of 60-Nitinol with surface treatment C (a) along with EDS spectra at the indicated locations (b) to (d).

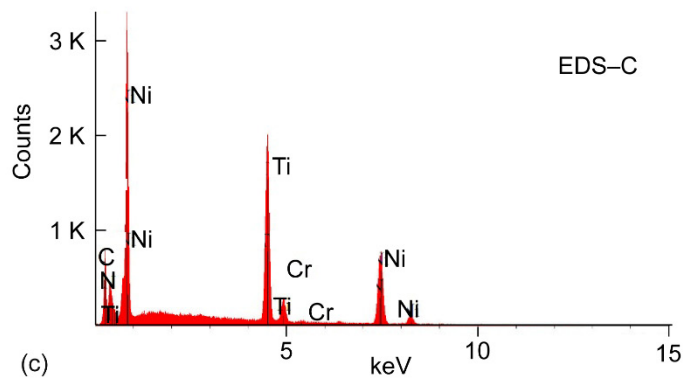
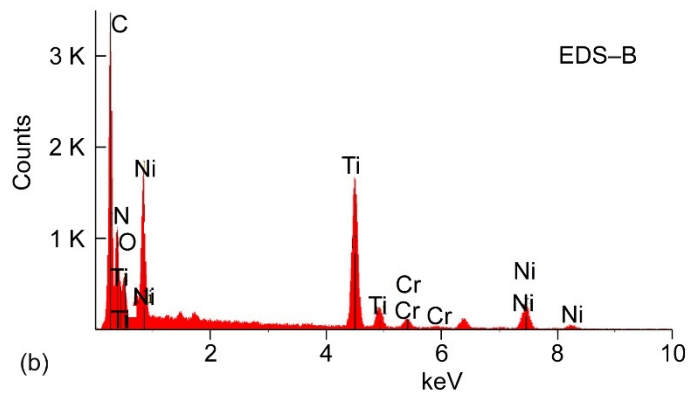
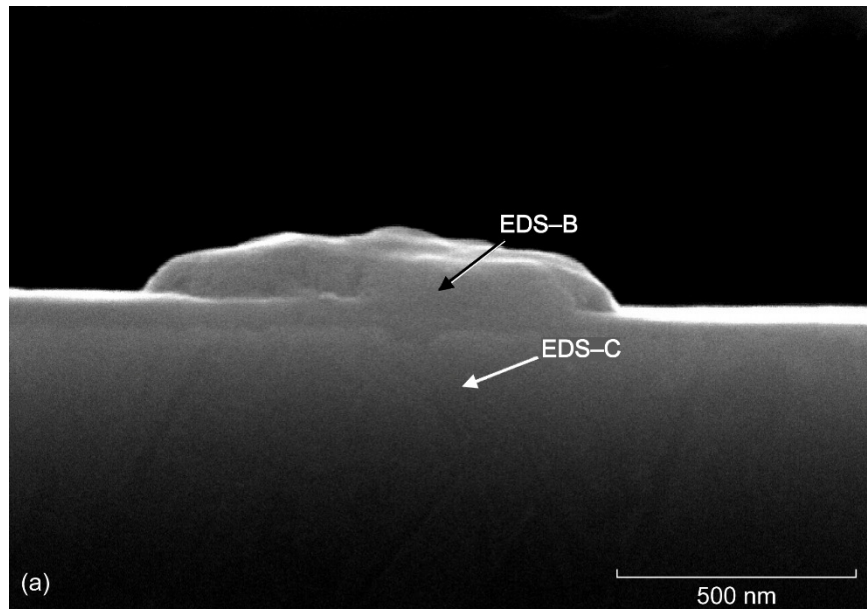


Figure 9.—SEM photomicrograph (a) and EDS spectra (b) to (c) from cross-section of 60-Nitinol after direct plasma nitriding (surface treatment D).

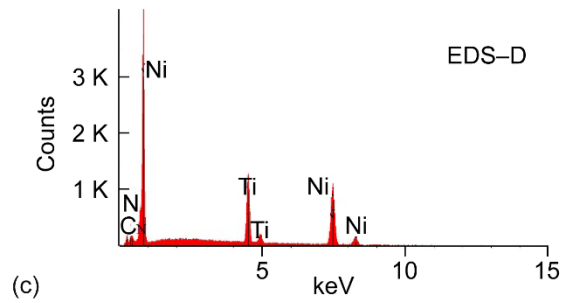
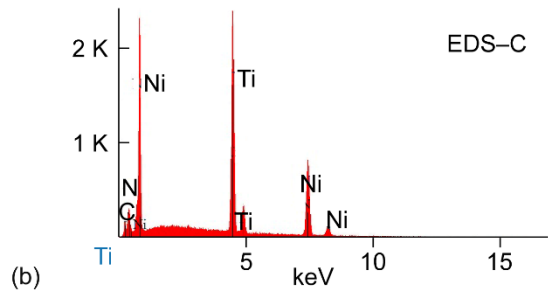
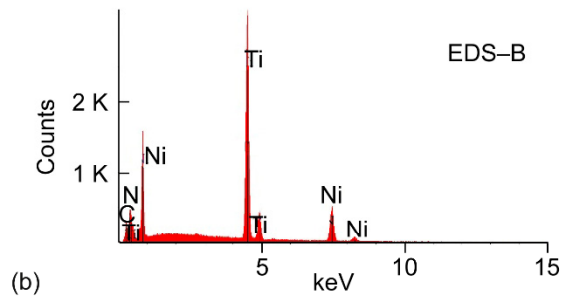
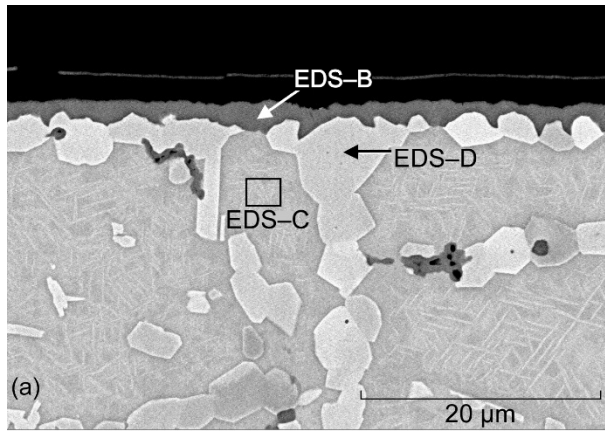


Figure 10.—SEM photomicrograph (a) and EDS spectra (b) to (d) from cross-section of 60-Nitinol after surface treatment E.

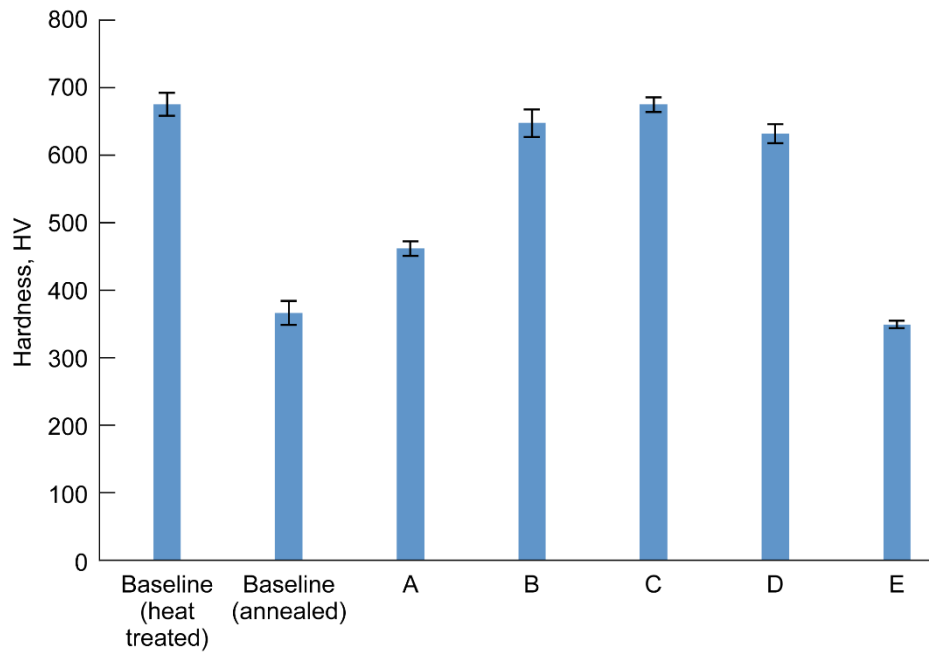


Figure 11.—Microindentation hardness of the substrate material.

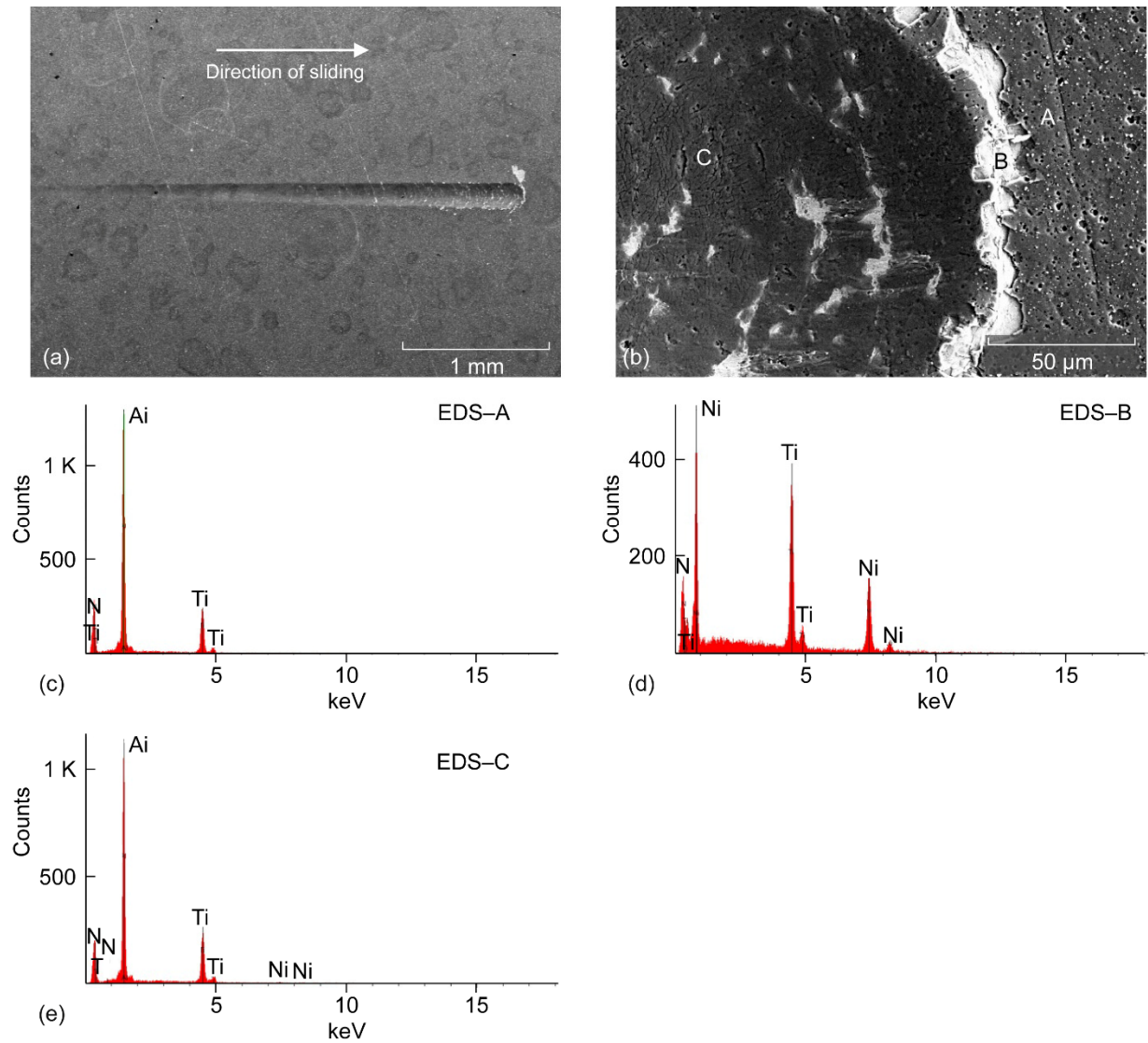


Figure 12.—SEM photomicrographs of (a) scratch channel and (b) higher-magnification view at end of scratch channel as well as EDS spectra at the areas (c) to (e) from Ti-Al-N PVD coating (surface treatment A) wear scar.

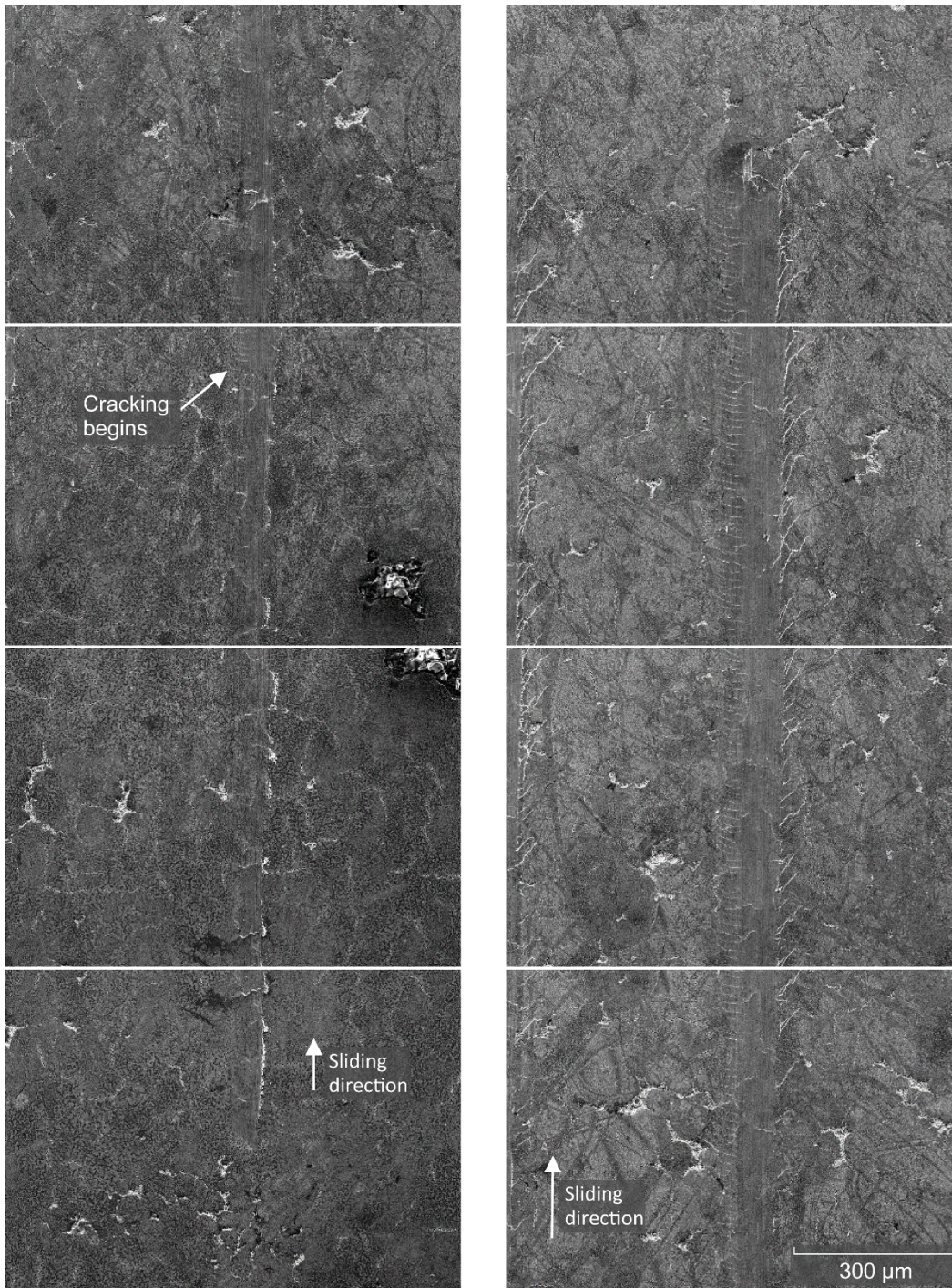


Figure 13.—Scratch channel on surface treatment B, showing low levels of cracking beginning where indicated (corresponding to a load of approximately 33 N).

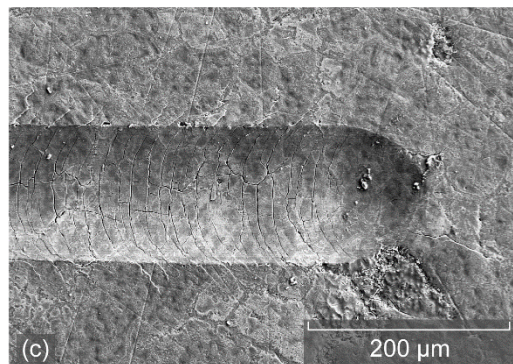
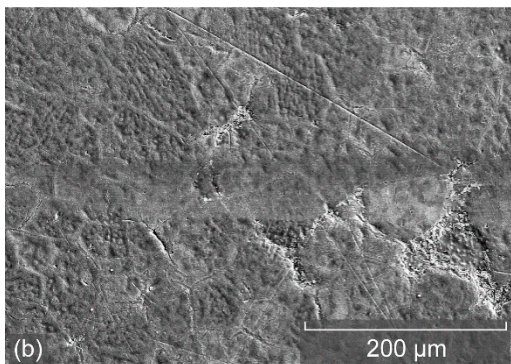
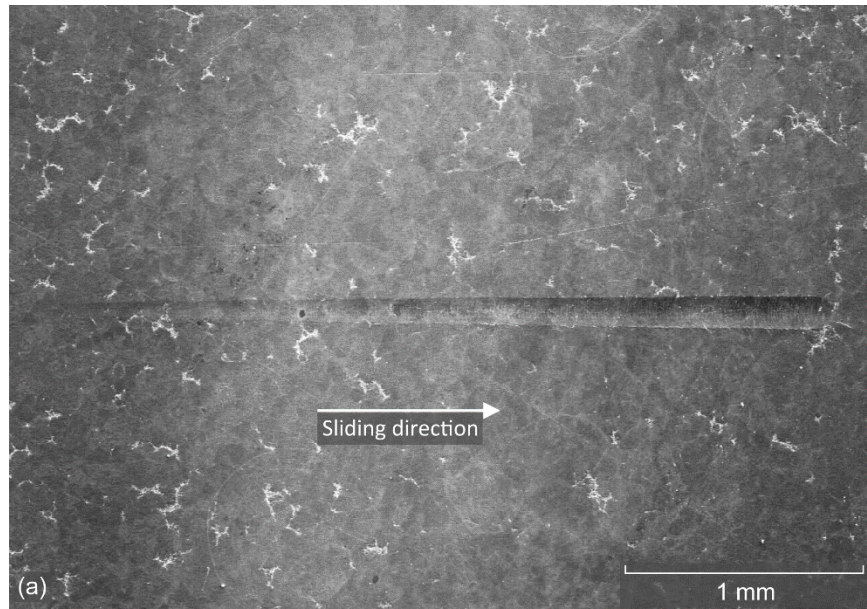


Figure 14.—Scratch channel on surface treatment C (gas nitride run M26758N) showing (a) entire scratch channel, (b) beginning of scratch channel and (c) end of scratch channel.

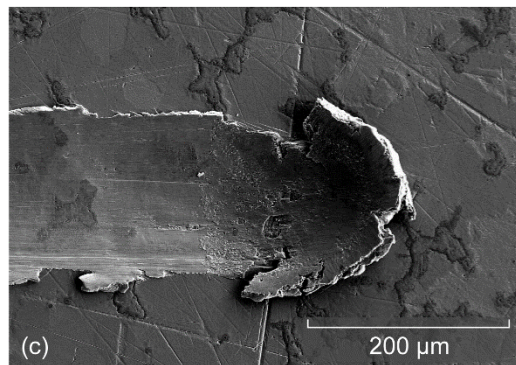
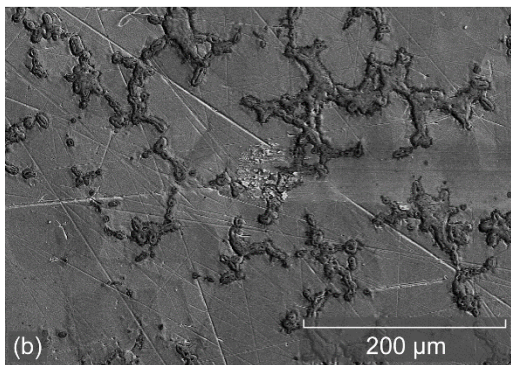
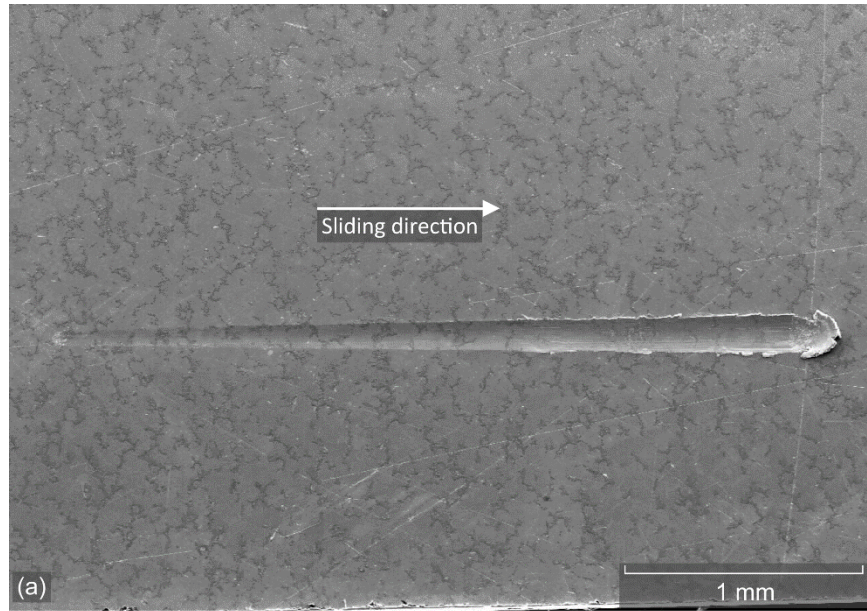


Figure 15.—SEM photomicrographs at (a) lower and (b) to (c) higher magnification of the scratch channel on surface treatment D (plasma nitride run M26728T). The start of the scratch channel is shown in b, while the end is shown in c. The surface treatment deforms plastically (see Fig. 15(c)) while remaining adherent to the surface.

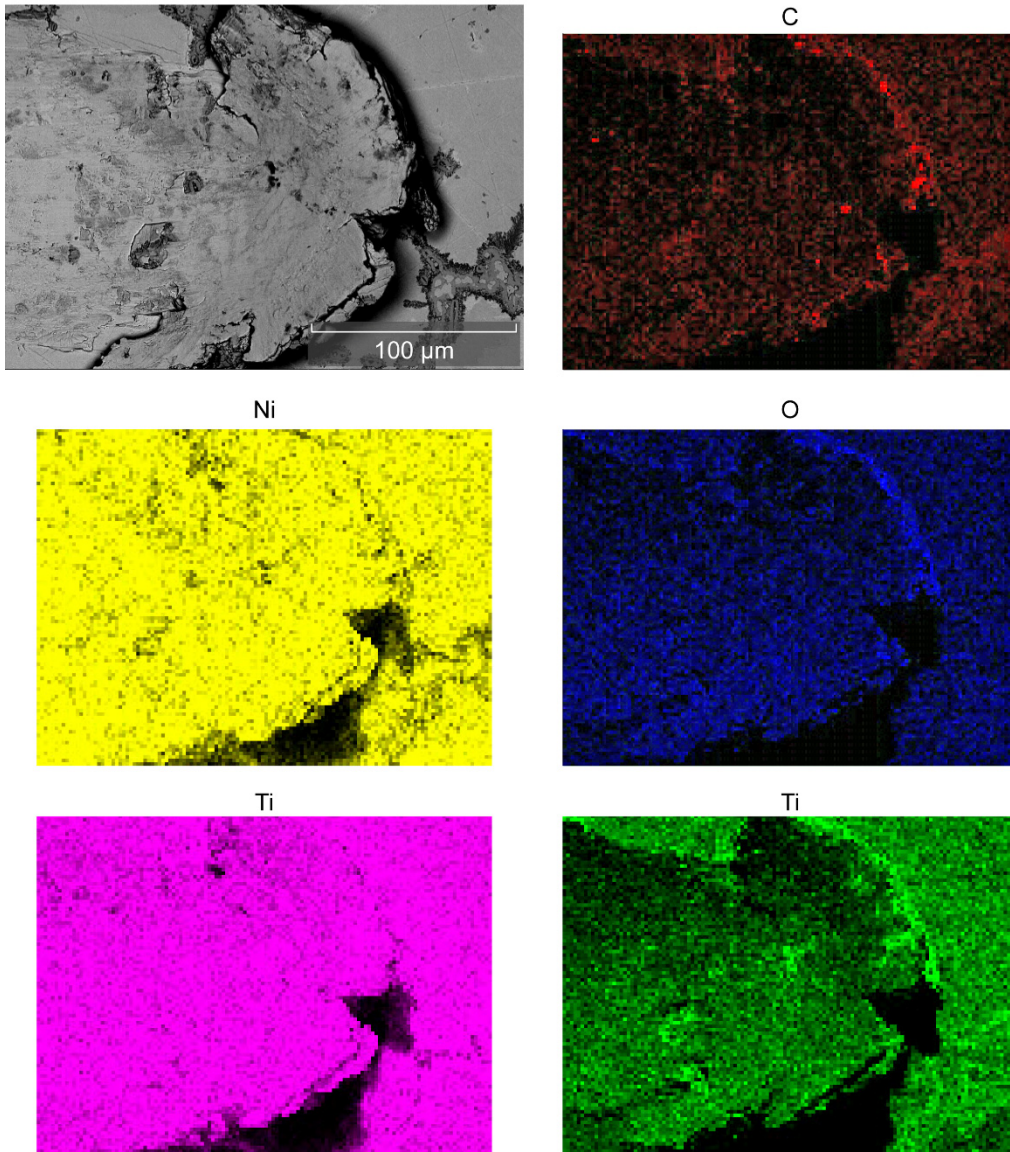


Figure 16.—SEM photomicrograph and elemental dot mapping at the end of the scratch scar on surface treatment D indicating a relatively even distribution of nickel, titanium, and nitrogen across the surface and in the scratch scar.

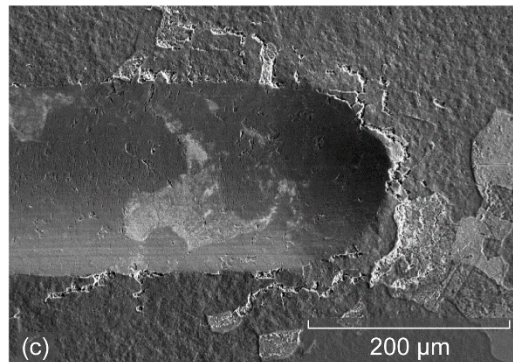
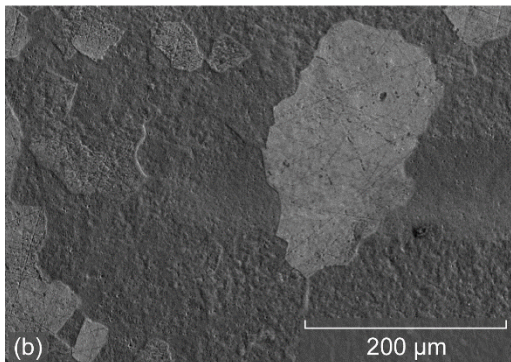
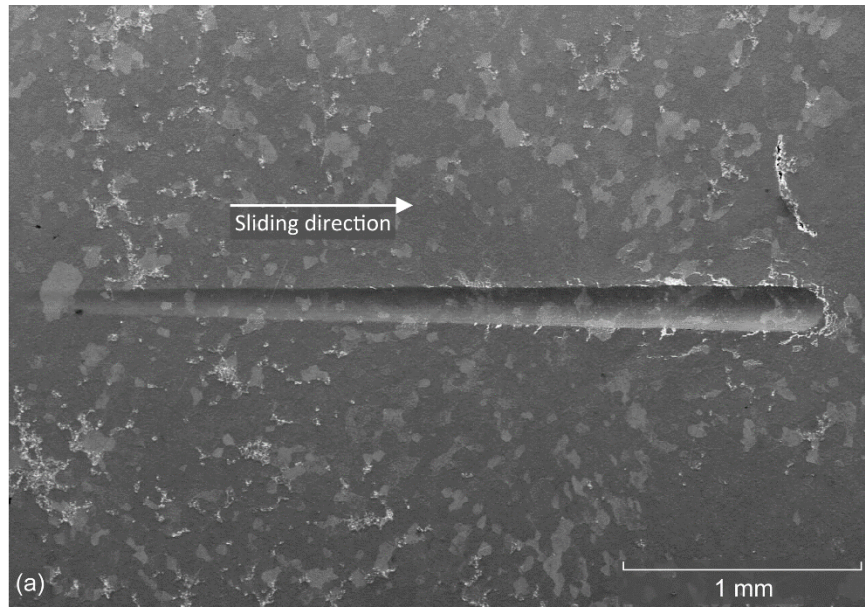


Figure 17.—SEM photomicrographs (a) lower and (b) to (c) higher magnification of the scratch scar on surface treatment E (indirect plasma nitride run 55613N). The start of the scratch channel is shown in (b), while the end is shown in (c). The surface treatment appears to separate slightly from the substrate near the termination of the scratch scar (see Fig. 17(c)) but appears to be adherent to the substrate elsewhere.

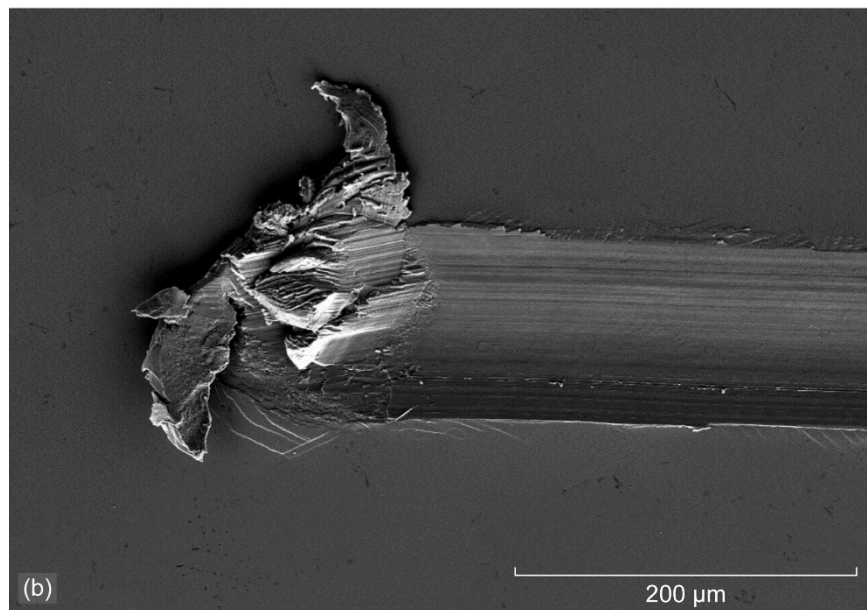
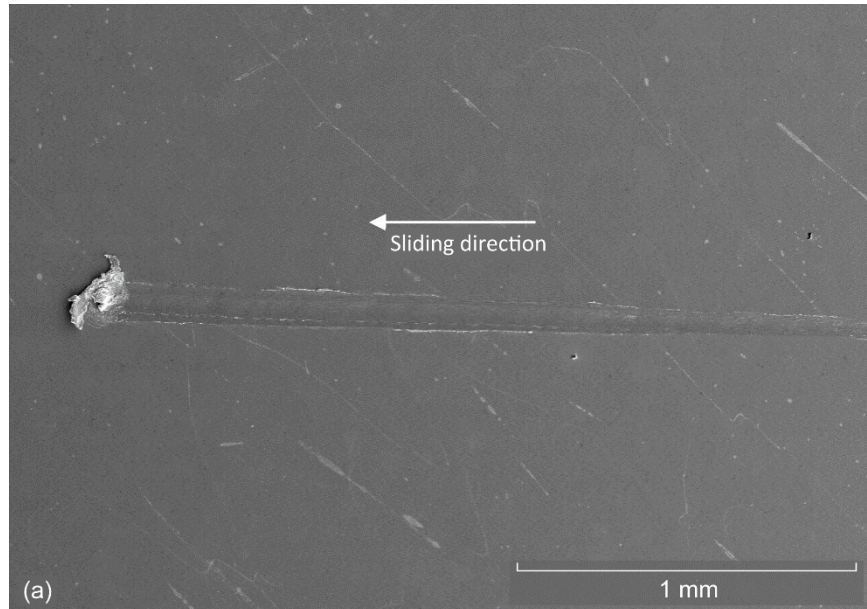


Figure 18.—Baseline scratch channel profile on untreated 60-Nitinol, hardened to 673HV at (a) low magnification and (b) higher magnification. The end of the scratch channel in (b) shows a mass of material that has been displaced by the diamond stylus, indicating abrasive wear.

